Sergei Rudenko, Mathis Bloßfeld, Horst Müller, Denise Dettmering, Detlef Angermann, and Manuela Seitz: **Evaluation of DTRF2014, ITRF2014, and JTRF2014 by Precise Orbit Determination of SLR Satellites**, *IEEE Transactions on Geoscience and Remote Sensing*, DOI: https://doi.org/10.1109/TGRS.2018.2793358, in print, 2018.

1 2

Evaluation of DTRF2014, ITRF2014 and JTRF2014 by Precise Orbit Determination of SLR Satellites

Sergei Rudenko, Mathis Bloßfeld, Horst Müller, Denise Dettmering, Detlef Angermann, and Manuela Seitz

***Abstract*—In 2016, three new realizations of the International Terrestrial Reference System (ITRS), namely DTRF2014, ITRF2014, and JTRF2014, have been released. In this paper, we evaluate these ITRS realizations for precise orbit determination of ten high and low Earth orbiting geodetic satellites using satellite laser ranging (SLR) observations. We show the reduction of observation residuals and estimated range biases, when using these new ITRS realizations, as compared to the previous ITRS realization for SLR stations – SLRF2008. Thus, the mean SLR root-mean-square (RMS) fits reduce (improve), on average over all satellites tested, by 3.0, 3.6, 8.1, and 7.7% at 1993.0 - 2015.0, when using ITRF2014, DTRF2014, DTRF2014 with non-tidal loading, and JTRF2014 realizations, respectively. The improvement of the RMS fits is even larger at 2015.0 - 2017.0: 14.0 and 15.5% using ITRF2014 and DTRF2014, respectively. For the altimetry satellite Jason-2, we found improvements in the RMS and mean of the sea surface height crossover differences with the new ITRS realizations, as compared to SLRF2008. We show that JTRF2014, after an editing done for SLR stations Conception and Zimmerwald, and DTRF2014 with non-tidal loading corrections result in smallest RMS and absolute mean fits of SLR observations indicating the best performance among the ITRS realizations tested, while using SLRF2008 and ITRF2014 causes a 0.2–0.3 mm/y trend in the mean of SLR fits at 2001.0–2017.0.**

***Index Terms*—Altimetry, DTRF2014, ITRF2014, Jason-2, JTRF2014, LAGEOS, orbit determination, satellite laser ranging (SLR), space geodesy, Starlette, terrestrial reference frames**

I. Introduction

The International Terrestrial Reference Frame (ITRF) is the realization of the International Terrestrial Reference System (ITRS) [26]. The ITRF is a global reference frame comprising positions and velocities of globally distributed space geodetic observation stations. High accuracy, consistency, and long-term stability is required for precise monitoring global change phenomena (e.g., global and regional sea level change, post-glacial rebound, tectonic motion and deformations), Earth's rotation as well as for precise positioning applications on and near the Earth's surface [2], [3].

The new ITRS realizations were published in 2016. They are ITRF2014 [1], DTRF2014 [36], and JTRF2014 [38]. These realizations are based on identical input data provided by the combination centers of the four space geodesy techniques (Doppler Orbitography and Radiopositioning Integrated by Satellite (DORIS), Global Navigation Satellite System (GNSS), Satellite Laser Ranging (SLR), and Very Long Baseline Interferometry (VLBI)) as a result of the reprocessing effort of each of the technique services: International DORIS Service (IDS, [37]), International GNSS Service (IGS, [12]), International Laser Ranging Service (ILRS, [25]), and International VLBI Service for Geodesy and Astrometry (IVS, [34]). However, the three ITRS realizations differ conceptually. While DTRF2014 and ITRF2014 provide station positions at a reference epoch and velocities, the JTRF2014 consists of weekly time series of station positions. Differences between the DTRF2014 and the ITRF2014 solutions result from different combination approaches applied by the ITRS combination centers and center-specific data editing steps such as, e.g., the handling of the local ties. As an example, [7] address the scale difference between the ITRF2014 and DTRF2014. For the sites affected by major earthquakes, the ITRF2014 provides, besides linear station motions, also post-seismic deformation (PSD) models, while the DTRF2014 uses a piecewise linear representation of station positions. Another difference is that within the DTRF2014 computation, atmospheric and hydrological non-tidal loading was applied, while within the ITRF2014 computation, post-fit multi-frequency (annual, semi-annual, etc.) correction models were estimated. These correction models are available on request from the IGN (Institut National de l'Information Géographique et Forestière) ITRS Product Centre of the International Earth Rotation and Reference Systems Service (IERS). Another principal difference between these three ITRS realizations is that station positions can be computed using DTRF2014 and ITRF2014 also outside the time span (1980.0 – 2015.0) where observations were involved in their creation, while the JTRF2014 can be used only at the time interval from 28 November 1979 to 14 February 2015. Therefore, we distinguish in our analysis between an interpolation time interval (1993.0 – 2015.0), where all TRF realizations are available, and an extrapolation time interval (2015.0 – 2017.0), where only the DTRF2014 and ITRF2014 solutions are available.

In case of the DGFI-TUM solution, the linear DTRF2014 solution is accomplished with the following time series files, necessary for the computation of the quasi-instantaneous station positions[1]:

1) Non-tidal loading (NTL) time series (denoted below as "NTL") in the form of weekly averaged atmospheric

Manuscript received May 22, 2017. This research was partly supported by German Research Foundation (DFG) within the projects "Consistent dynamic satellite reference frames and terrestrial geodetic datum parameters", "Interactions of low-orbiting satellites with the surrounding ionosphere and thermosphere (INSIGHT)". (*Corresponding author: Sergei Rudenko.*)

The authors are with Deutsches Geodätisches Forschungsinstitut, Technische Universität München (DGFI-TUM), 80333 Munich, Germany, e-mail: sergei.rudenko@tum.de, mathis.blossfeld@tum.de, horst.mueller@tum.de, denise.dettmering@tum.de, detlef.angermann@tum.de, manuela.seitz@tum.de

[1] http://www.dgfi.tum.de/fileadmin/w00btu/www/DTRF2014_readme.pdf

and hydrological non-tidal loading corrections applied a posteriori at the normal equation (NEQ) level [35] in the DTRF2014 computation for the correction of the respective signals. The data are provided by Tonie van Dam and are based on the NCEP atmosphere model [18] and the GLDAS hydrology model [29];

2) Station position residuals (denoted below as "Res") being transformation residual time series obtained from similarity transformations of the technique-specific epoch-wise solutions with respect to DTRF2014;
3) Translation time series of the origin (denoted below as "Ori") derived from similarity transformations of SLR-only 15-day/weekly network solutions with respect to DTRF2014.

Moreover, since the station residuals and the SLR-only translation time series depend on the specific solution setup applied for DTRF2014, we recommend to use the DTRF2014 linear station motion model and, if favored, the geophysical non-tidal atmospheric and hydrological loading corrections. A summary of the new ITRS realizations is given in Table I.

In this paper, we evaluate the most recent ITRS solutions for precise orbit determination (POD) of ten geodetic satellites equipped with SLR retro-reflectors at high (with an altitude more than 2000 km) and low (with an altitude below this value) Earth orbits (HEO and LEO, respectively) in total over 24 years from 1993.0 to 2017.0 using SLR-only orbit determination. We have chosen LAGEOS-1/2, since these are the core geodetic satellites. They, together with Etalon-1/2, are used for the TRF and Earth Orientation Parameters (EOP) determination within the ILRS [21]. SLR data of LARES and LAGEOS-1/2 satellites are used for general relativity tests, e.g. [10]. Using SLR data of spherical geodetic satellites, such as Ajisai, Etalon-1/2, LAGEOS-1/2, Larets, Starlette, and Stella in combination with GRACE data was shown [16] can improve the low degree coefficients of the Earth's gravity field that are not reliably derived from pure GRACE measurements. We have chosen also a non-spherical satellite Jason-2 that serves as one of the altimetry reference missions for sea level investigations [27]. We derive Jason-2 orbit between 20 July 2008 and 1 March 2015, where the major improvements were expected and found, as compared to using the previous ITRS realization for SLR stations – SLRF2008 (version of 8 August 2016) [24]. We use all these satellites located at the altitudes from 681 to 19125 km above the Earth, with orbit inclinations from 49.8° to 109.8°, since each satellite reacts to an ITRS realization in its own way. We compare the results with those obtained using the SLRF2008.

The rest of the paper is organized as follows. The applied approach is described in Section II. Since ITRS realizations directly impact station positions, we show in Section III the impact of the ITRS realizations on weekly estimated mean range biases and separately on pass-wise estimated range biases for some stations of the SLR network. The influence of the ITRS realizations on the root-mean-square (RMS) and mean fits of SLR observations of ten geodetic satellites and orbit differences for Jason-2 is provided in Section IV. The effect of the ITRS realizations on Jason-2 radial and geographically correlated errors as well as RMS and mean of the sea surface height crossover differences is shown in Section V. Finally, conclusions are drawn in Section VI.

II. The approach

To quantify the impact of the new ITRS realizations, we employed the DGFI Orbit and Geodetic parameter estimation Software (DOGS-OC; [15], [5]) for precise orbit determination of the selected satellites using SLR observations and by applying three various ITRS realization: DTRF2014, ITRF2014, and JTRF2014. In case of DTRF2014, we test, besides the linear DTRF2014 realization, also that one with atmospheric and hydrological non-tidal loading (DTRF2014+NTL).

In case of JTRF2014, one obtains unrealistic fits of SLR observations (3.5 times larger than those derived using two other new ITRS realizations), when using JTRF2014 as it is. However, observation fits become realistic after the exclusion of SLR station Concepcion (CDDIS SOD 74057903, IERS DOMES number 41719M001) after 27 February 2010, since no jump caused by Maule earthquake ($M_w = 8.8$) took place on this day is provided in the positions of this station in the JTRF2014. Additionally, JTRF2014 provides two solutions for station Zimmerwald (CDDIS SOD 78106801, IERS DOMES numbers 14001S001 and 14001S007) at the whole time interval. We use solution A (DOMES number 14001S001) before 30 April 1995 and solution B (DOMES number 14001S007) after this date. We use the accordingly corrected JTRF2014 realization in this paper.

We compute satellite orbits by numerical integration of differential equations of motion by taking into account gravitational and non-gravitational forces acting on the satellites. In all tests, the same background models and input data (Table II) are used for the POD to ensure that orbit differences are only caused by the different ITRS realizations applied. All above mentioned ITRS realizations are used with the same (IERS EOP 08 C04) series of the Earth orientation parameters being an official IERS EOP product.

At each orbital arc, six Keplerian elements, one solar radiation pressure coefficient and one Earth albedo and infrared radiation pressure coefficient are estimated. Additionally, atmosphere drag coefficients are estimated with 12 h step for LEO satellites and none for HEO satellites. Besides, we estimate transversal and normal once-per-revolution (OPR) cosine and sine empirical accelerations once per arc for all satellites and transversal empirical accelerations once per day for HEO satellites. Since the area-to-mass ratio of Ajisai is about 5.5 times larger than that one of Starlette and Stella, while the Ajisai altitude is about twice higher than that one of two these satellites, the same parameterization of the atmosphere drag coefficients and empirical accelerations is used for these satellites. We estimate separately weekly and pass-wise station-specific range biases of all stations in two tests described in Section III, but do not estimate any range and time biases for the results shown in Sections IV-V. We apply range, time, and atmosphere pressure biases to the SLR tracking data of the stations, satellites, and periods specified in the ILRS Analysis Standing Committee data handling

TABLE I
A SHORT SUMMARY ON THE ITRF2014, DTRF2014 AND JTRF2014

Solution	ITRF2014	DTRF2014	JTRF2014
Institute	IGN (Paris, France)	DGFI-TUM (Munich, Germany)	JPL (Pasadena, USA)
Software	CATREF	DOGS-CS	CATREF + KALMAN
Combination approach	Solution (parameter) level	Normal equation level	Solution (parameter) level
Station position	Position $\mathbf{X}_{\mathbf{ITRF}}(t_0)$ + velocity $\dot{\mathbf{X}}_{\mathbf{ITRF}}(t_0)$ + PSD model (for selected stations) + annual signals (on request)	Position $\mathbf{X}_{\mathbf{DTRF}}(t_0)$ + velocity $\dot{\mathbf{X}}_{\mathbf{DTRF}}(t_0)$ + NTL models + SLR origin + residual station motions	Weekly positions $\tilde{\mathbf{X}}_{\mathbf{JTRF}}(t_i)$

recommendation file[2]. No station coordinates are estimated in this study. Moreover, we do not apply station-dependent weighting, i.e. do not distinguish between the ILRS core (best quality) and non-core (other) stations in the POD, to ensure a clear interpretation of the results.

We investigate the impact of the ITRS realizations on the following control parameters: weekly and pass-wise estimated mean station-specific range biases, RMS and mean fits of SLR observations, as well as RMS and mean of single-satellite sea surface height crossover differences. Since we use the same observations and the same background POD models, and apply the same parameterization to test each ITRS realization, the smallest absolute values of each of the control parameters indicate that the respective ITRS realization performs best among the tested realizations. The ITRF2014 is used as it is, i.e., including post-seismic deformation models for stations, for which they are provided. Within the extrapolation time period, only the conventional linear station motion model was available for the DTRF2014 solution. This means, the linear DTRF2014 is compared to the ITRF2014 (linear plus PSD models) and the most recent update of the SLRF2008.

III. Impact on the weekly and pass-wise estimated mean station-specific range biases

ITRS realizations provide station positions that can be generally used to compute or estimate station heights. Fig. 1 shows four extreme cases of the height of the ILRS stations computed with respect to common mean values. The ITRS realizations give heights that differ by up to several cm with respect to each other within the interpolation interval. Moreover, they show significant discrepancies in the extrapolation interval which accumulate with time.

Using SLR observations to two LAGEOS satellites in $1993-2014$ [4] showed that systematic, not properly treated and interpreted range errors at some stations contributing to the TRF determination can cause errors in the scale of this reference frame derived from the SLR technique. Therefore, to evaluate the quality of the different ITRS realizations, we use SLR observations and analyze weekly estimated range biases for stable (core) stations of the SLR network. Within the analysis, the station positions are fixed to the respective ITRS realization. The mean weekly biases for the core stations obtained using LAGEOS-1 observations are shown for the extrapolation time period in Fig. 2. For the interpretation of this figure, it has to be mentioned that in the reprocessing for the TRF input, the ILRS Analysis Centers are requested to apply range biases reported in the ILRS Analysis Standing Committee data handling recommendation file (see Sect. II). Therein, for Fort Davis (7080), Zimmerwald (7810), Graz (7839), Herstmonceaux (7840), and Matera (7941), biases are reported. However, since for none of the stations shown in Fig. 2 any range bias is reported in the extrapolation time interval, only zero range biases are expected and the smallest estimated range biases indicate the best-performing TRF solution. The diverse velocities of Arequipa (Fig. 1) clearly affect the estimated range biases (Fig. 2). In general, the SLRF2008 causes the largest range biases. This is due to the fact that SLRF2008 was derived using data only until 2009.0, while the latest ITRS realizations were derived using the data until 2015.0 and, therefore, more precisely provide station motions after 2009.0, than their predecessors. The radial error in station positions increasing with time after 2009.0 when using SLRF2008 (see also Sect. IV) causes increased range biases, when estimated. The DTRF2014 solution causes some smaller range biases in Europe whereas the ITRF2014 performs slightly better in the southern hemisphere.

As shown in Fig.1, the height for Komsomolsk (Russia) ILRS station differs significantly after 2015.0. We have performed another test in which we estimated pass-wise range biases of all SLR stations, including Komsomolsk. Fig. 3 exemplarily shows the pass-wise estimated range biases for this station obtained using LAGEOS-1 and LAGEOS-2 observations for the three ITRS realizations. Whereas the mean offset between the range biases obtained using DTRF2014 and ITRF2014 is below $5-9$ mm, the offset w.r.t. the SLRF2008 already increased to $4-6$ cm within the two years of the extrapolation time period. The mean values of the estimated range biases show that DTRF2014 performs better than ITRF2014 and SLRF2008 performs worse than both. Komsomolsk serves as an example of an extreme case in this study. For other SLR stations, the differences between the ITRF2014 and the DTRF2014 are generally smaller for both LAGEOS satellites and result in about 1.2 mm (global mean) larger range biases for ITRF2014 w.r.t. DTRF2014 and about 6.3 mm larger range biases for SLRF2008 w.r.t. DTRF2014.

[2]https://ilrs.dgfi.tum.de/fileadmin/data_handling/ILRS_Data_Handling_File.snx

TABLE II
THE MAIN BACKGROUND MODELS AND INPUT DATA USED FOR PRECISE ORBIT DETERMINATION

Reference system	
Polar motion and UT1	IERS EOP 08 C04 (IAU2000A) series with sub-daily oceanic tide model of Ray
Precession and nutation model	IAU2000A [26]
Force models	
Earth gravity field model	EIGEN-6S [13], up to n=m=30 for HEO and n=m=120 for LEO satellites
Third body attraction	Sun, Moon, Jupiter, Venus, Saturn, Mars, Mercury (DE-421, [14])
Moon gravity field model	Konopliv [20], up to n=m=10
Solid Earth tide model	IERS Conventions (2010) [26]
Solid Earth pole tide model	IERS Conventions (2010) [26]
Ocean tide model	EOT11a [33], up to n=m=120, full tidal admittance
Ocean pole tide	[11]
Atmospheric density model	CIRA-86 [17] for Jason-2, JB2008 [9] for other LEO, none for HEO satellites
Earth albedo and infrared radiation pressure	Knocke CSR model [19]
Solar radiation pressure	DOGS-OC models: spherical for spherical satellites and box/wing for Jason-2
Empirical accelerations	Adjusted (see Section II)
Relativistic corrections	post-Newtonian (Schwardshild, Lense-Thirring, and de Sitter, [26])
Displacement of the reference points	
Solid Earth tidal displacement	IERS Conventions (2010) [26]
Solid pole tide displacement	IERS Conventions (2010) [26]
Ocean loading	EOT11a
Ocean pole tide displacement	[11]
Tidal atmospheric loading	Ray-Ponte model [28]
Mean pole	IERS Conventions (2010) [26]
Measurements, arcs	
SLR measurements	from NASA CDDIS and EDC ILRS data centers
System-dependent center-of-mass correction	[22], [23]
Arc length	7 days, but 3.5 days for Jason-2
Satellite attitude	quaternions for Jason-2, if available, otherwise Jason-2 nominal yaw-steering model

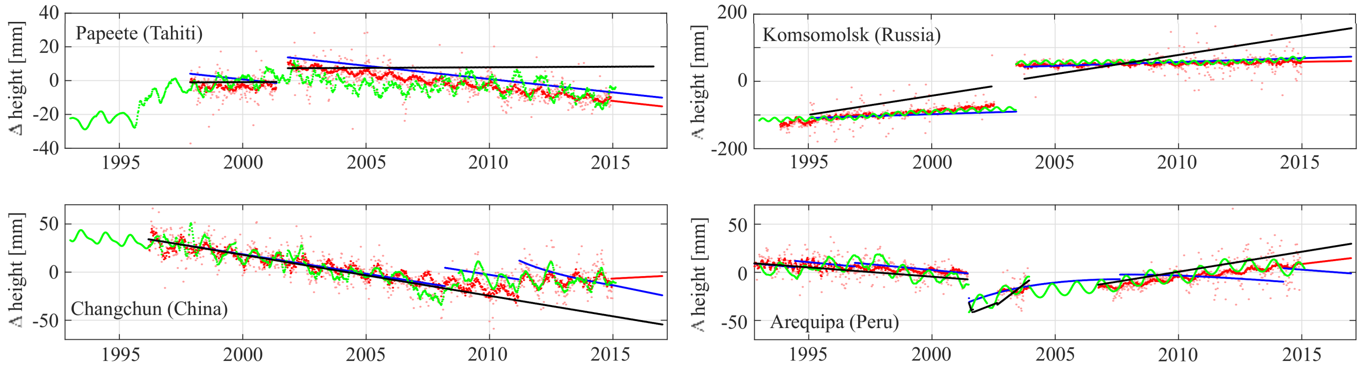

Fig. 1. Height time series (in mm: common mean subtracted) of the ILRS stations Papeete (Tahiti), Changchun (China), Komsomolsk (Russia), and Arequipa (Peru) for the interpolation interval (1993.0 – 2015.0) and the extrapolation interval (2015.0 – 2017.0) from four different ITRS realizations: most recent SLRF2008 (black), ITRF2014 (blue), DTRF2014+NTL (red), and JTRF2014 (green). In addition, the solution DTRF2014+Res+Ori+NTL (light red) is shown in the background. Note: no seasonal, annual, or semi-annual corrections are applied within the extrapolation interval.

IV. IMPACT ON SATELLITE ORBITS, RMS, AND MEAN FITS OF SLR OBSERVATIONS

The impact of DTRF2014, ITRF2014, and JTRF2014 on the RMS and mean values of residuals of SLR observations of ten geodetic satellites is shown in Tables III and IV, respectively. A bit higher level of the RMS fits of SLR observations shown in Table III than that one obtained by the ILRS analysis centers and POD groups during the TRF and EOP determination e.g. in [32] and [39] is, since we do not estimate in this study neither station coordinates, nor EOP, nor range biases, but use only SLR observations, apply the same weighting of observations of all stations in the POD process, and estimate OPR cosine and sine empirical accelerations in the along- and cross-track directions once per arc to investigate the impact of various ITRS realizations on observation residuals.

For the interpolation time period, the smallest RMS fits and the smallest absolute values of mean fits of SLR observations are obtained using JTRF2014 and DTRF2014+NTL, since both realizations provide non-linear station motions for all stations included in each of them. One should notice that the filter noise for the JTRF2014 Kalman filter was calibrated with respect to atmospheric, oceanic and hydrological non-tidal loading, whereas the DTRF2014+NTL reference frame contains only atmospheric and hydrological non-tidal loading corrections. The JTRF2014 possibly approximate also other non-linear station motions resulting in better fits.

For the extrapolation time period, DTRF2014 provides smaller RMS fits and the smallest absolute values of mean fits of SLR observations than ITRF2014 and SLRF2008 for the most satellites tested. The largest RMS fits and absolute

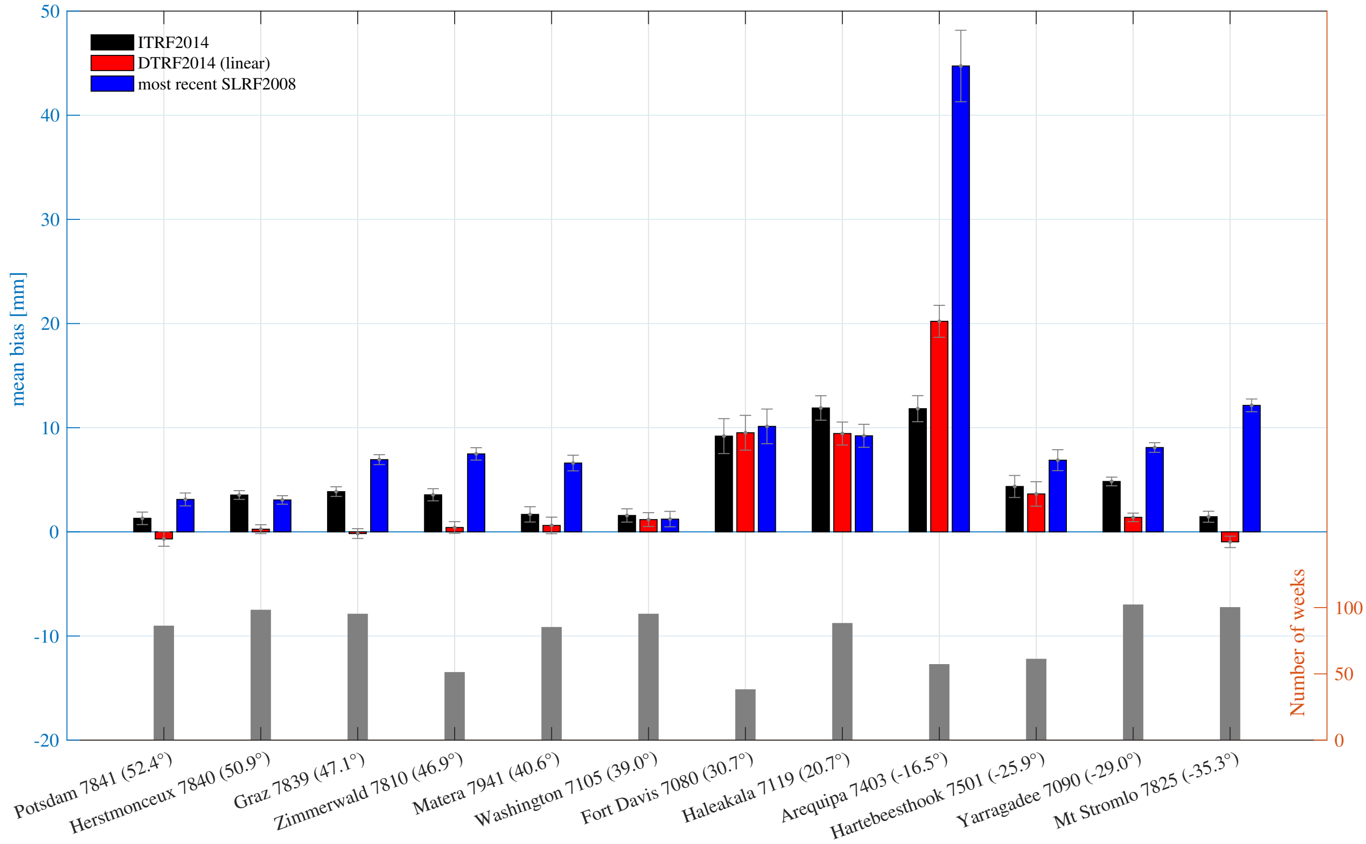

Fig. 2. Estimated mean station-specific weekly range biases (in mm) and their error bars for ILRS core stations obtained using different ITRS realizations in the extrapolation time period for LAGEOS-1. In addition, the number of processed weeks is shown for each station.

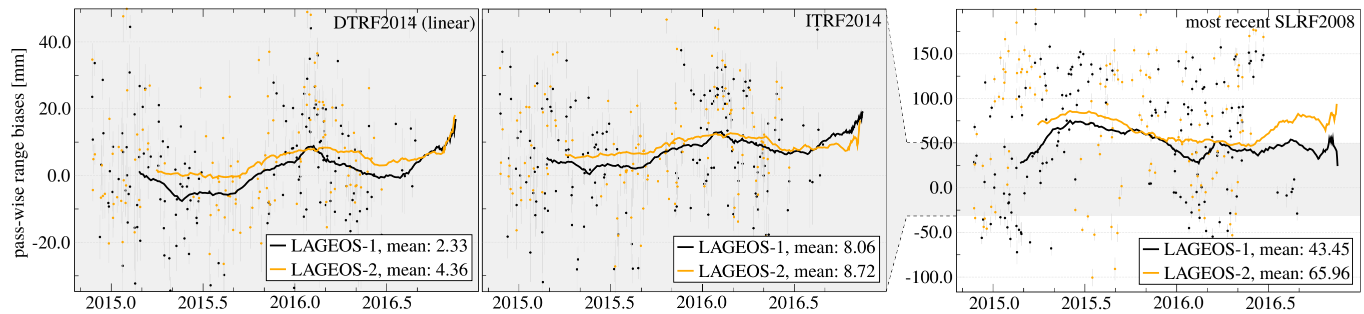

Fig. 3. Estimated pass-wise range biases (in mm) of the ILRS station Komsomolsk (Russia) for different ITRS realizations in the extrapolation period. Note the different scale for the range biases for the SLRF2008 (right plot).

mean fits of observations are obtained using SLRF2008 for most satellites tested, since SLRF2008, on the contrary to other ITRS realizations studied here, provides extrapolated station positions beyond 2009.0. Since JTRF2014 is available only until 14 February 2015, no results are provided in Tables III-IV for the extrapolation period for this reference frame. Generally larger mean fits of SLR observations obtained for Ajisai ($1.2-1.7$ cm) than for the other nine satellites might be caused by the deficiencies in the system-dependent center-of-mass corrections [22] used for this satellite. The same conclusion is made by [6], who show that adding Ajisai to a four-satellite constellation of LAGEOS-1/2 and Etalon-1/2 degrades the z-translation and the scale of TRF determination.

To investigate the temporal behavior of the RMS and mean fits of SLR observations, we chose LAGEOS-1 and Starlette as representatives of HEO and LEO satellites, respectively, since both missions completely cover the study period 1993.0 – 2017.0. Moreover, we use 50-week running averages to get rid of short-periodic fluctuations. We have tested different periods to compute running averages and found that the 50-week period being close to a yearly period shows most clearly the impact on the results. The time series of 50-week running averages of the RMS and mean fits of SLR observations for LAGEOS-1 and Starlette derived using four ITRS realizations (Fig. 4–7) show that the smallest RMS fits and the smallest absolute mean fits of observations are obtained using JTRF2014 and DTRF2014+NTL. The SLRF2008 shows the largest SLR RMS fits after 2009.0. The ITRF2014 and SLRF2008 show

TABLE III

MEAN VALUES OF RMS FITS OF SLR OBSERVATIONS (IN CM) OBTAINED USING VARIOUS TRF REALIZATIONS FOR TWO PERIODS: 1993.0 − 2015.0 AND 2015.0 − 2017.0. THE SMALLEST (BEST) VALUES FOR EACH SATELLITE AND EACH PERIOD ARE MARKED IN BOLD.

	LAGEOS-1	LAGEOS-2	Etalon-1	Etalon-2	LARES	Larets	Ajisai	Starlette	Stella	Jason-2
Time span 1993.0–2015.0										
SLRF2008	1.72	1.72	2.59	2.52	3.07	4.34	3.81	3.59	4.08	2.42
ITRF2014	1.63	1.62	2.56	2.48	2.85	4.30	3.77	3.27	4.07	2.28
DTRF2014	1.62	1.62	2.54	2.48	2.83	4.30	3.70	3.16	4.05	2.24
DTRF2014+NTL	**1.47**	**1.48**	2.53	2.47	**2.82**	4.21	3.65	**3.11**	3.35	2.24
JTRF2014	1.55	1.57	**2.49**	**2.44**	2.83	**4.20**	**3.64**	3.17	**3.32**	**2.20**
Time span 2015.0–2017.0										
SLRF2008	2.31	2.35	2.92	3.18	3.50	**5.73**	3.85	3.96	5.06	
ITRF2014	1.48	1.62	2.49	2.86	3.20	**5.73**	3.42	3.65	**4.74**	
DTRF2014	**1.41**	**1.52**	**2.44**	**2.82**	**3.19**	**5.73**	**3.31**	**3.64**	**4.74**	

TABLE IV

MEAN VALUES OF MEAN FITS OF SLR OBSERVATIONS (IN CM) OBTAINED USING VARIOUS TRF REALIZATIONS FOR TWO PERIODS: 1993.0 − 2015.0 AND 2015.0 − 2017.0. THE SMALLEST (BEST) ABSOLUTE VALUES FOR EACH SATELLITE AND EACH PERIOD ARE MARKED IN BOLD.

	LAGEOS-1	LAGEOS-2	Etalon-1	Etalon-2	LARES	Larets	Ajisai	Starlette	Stella	Jason-2
Time span 1993.0-2015.0										
SLRF2008	0.10	0.18	0.18	0.21	0.11	0.26	1.31	0.10	**0.00**	0.06
ITRF2014	0.12	0.19	0.19	0.22	**0.05**	0.25	1.33	0.12	0.03	0.08
DTRF2014	0.03	0.08	0.12	0.15	-0.15	**0.07**	**1.16**	-0.05	-0.13	**-0.04**
DTRF2014+NTL	**-0.02**	0.03	0.12	0.16	-0.13	**0.07**	**1.16**	-0.05	-0.14	**-0.04**
JTRF2014	-0.03	**0.02**	**0.09**	**0.13**	-0.13	**0.07**	**1.16**	**-0.04**	-0.10	**-0.04**
Time span 2015.0-2017.0										
SLRF2008	0.20	0.41	0.38	0.40	0.24	0.21	1.69	0.33	0.22	
ITRF2014	0.24	0.38	0.32	0.32	0.19	0.19	1.54	0.21	0.14	
DTRF2014	**0.00**	**0.11**	**0.20**	**0.19**	**-0.01**	**0.02**	**1.35**	**0.02**	**-0.06**	

a trend of 0.16 mm/y and 0.28 mm/y in the mean fits of observations for LAGEOS-1 and Starlette, respectively, at the time interval from 2001.0 to 2017.0. This might be caused by the worse approximation of the long-term SLR station coordinates which also results in larger range biases for many stations in the extrapolation interval when using ITRF2014 and SLRF2008, as compared to using DTRF2014 (see Fig. 2). Both TRFs, ITRF2014 and SLRF2008, produce a similar temporal behaviour of the SLR mean fits for Starlette (non-linear variation) with an offset from those ones obtained using JTRF2014, DTRF2014, and DTRF2014+NTL.

The 50-week running averages of the RMS and mean fits of SLR observations obtained for Jason-2 orbits using various ITRS realizations are shown in Fig. 8 and Fig. 9, respectively. The SLRF2008 provides the largest RMS fits of observations of this satellite since 2010.2, while the JTRF2014 gives the smallest RMS fits of SLR observations since 2010.3 among the four ITRS realizations tested. A jump in the SLR RMS fits obtained using ITRF2014 is found for Jason-2 after 2014.4. Again, as for Starlette, the 50-week running averages of the mean fits of SLR observations for Jason-2 show that the curve for ITRF2014 is close to the curve for SLRF2008 with the mean values of 0.08 and 0.06 cm, respectively, while the curves for DTRF2014, DTRF2014+NTL and JTRF2014 are close to each other providing the mean values of −0.03 and −0.04 cm, respectively (Fig. 9). Thus, DTRF2014, DTRF2014+NTL and JTRF2014 provide about twice closer to zero mean fits of SLR observations, than ITRF2014 and SLRF2008.

To investigate the impact of various ITRS realizations on satellite orbits, we compute radial differences of Jason-2 positions derived using these realizations. We chose Jason-2,

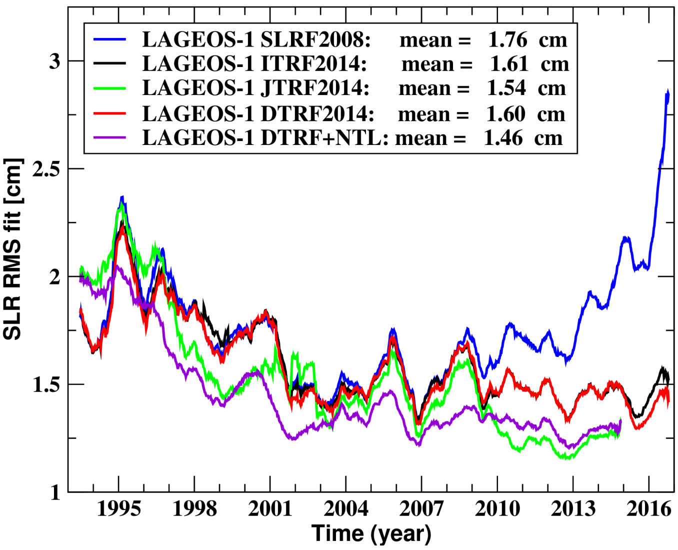

Fig. 4. 50-week running averages of the RMS fits of SLR observations (in cm) for LAGEOS-1 orbits derived using SLRF2008, ITRF2014, JTRF2014, DTRF2014 linear, and DTRF2014+NTL.

since this LEO satellite covers a time span after 2008, i.e. after SLRF2008 was created, and because Jason-2 is one of the most observed LEO satellites by SLR. Fig. 10 and Fig. 11 illustrate the radial differences of Jason-2 positions derived using DTRF2014, DTRF2014+NTL, ITRF2014, JTRF2014, and SLRF2008. Using SLRF2008 for Jason-2 POD results in increasing with time radial differences of satellite positions as compared to using DTRF2014, ITRF2014, and JTRF2014 (Fig. 10), since, in case of using SLRF2008, station positions at the time span beyond 2009.0 are computed by the

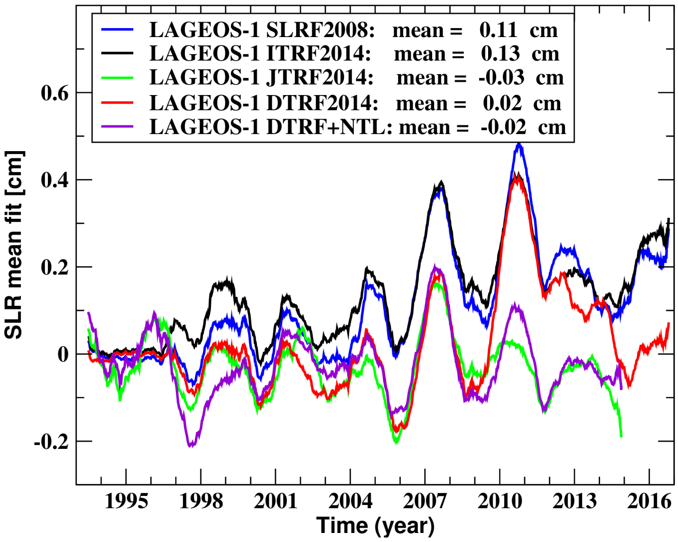

Fig. 5. 50-week running averages of the mean fits of SLR observations (in cm) for LAGEOS-1 orbits derived using SLRF2008, ITRF2014, JTRF2014, DTRF2014 linear, and DTRF2014+NTL.

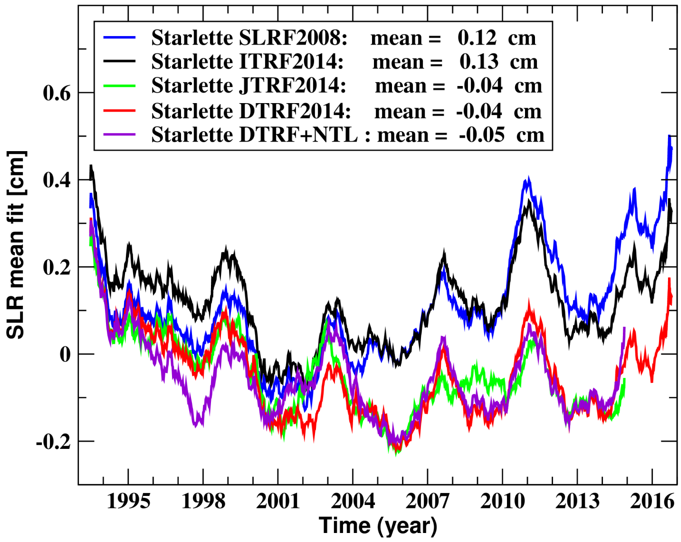

Fig. 7. 50-week running averages of the mean fits of SLR observations (in cm) for Starlette orbits derived using SLRF2008, ITRF2014, JTRF2014, DTRF2014 linear, and DTRF2014+NTL.

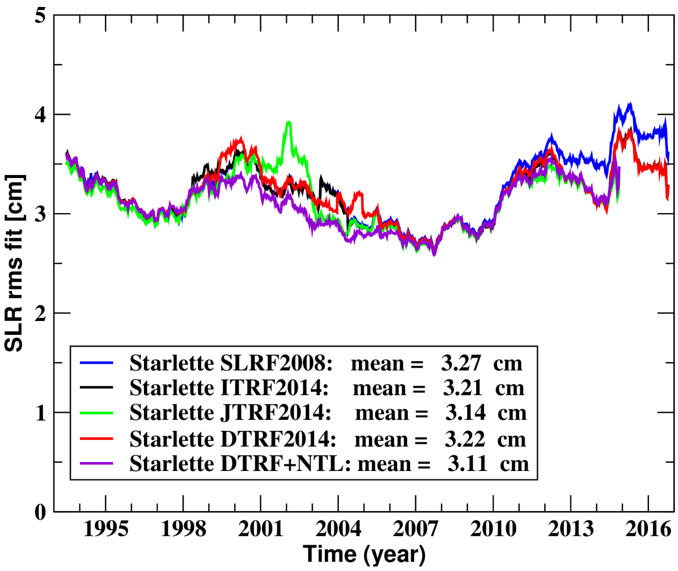

Fig. 6. 50-week running averages of the RMS fits of SLR observations (in cm) for Starlette orbits derived using SLRF2008, ITRF2014, JTRF2014, DTRF2014 linear, and DTRF2014+NTL.

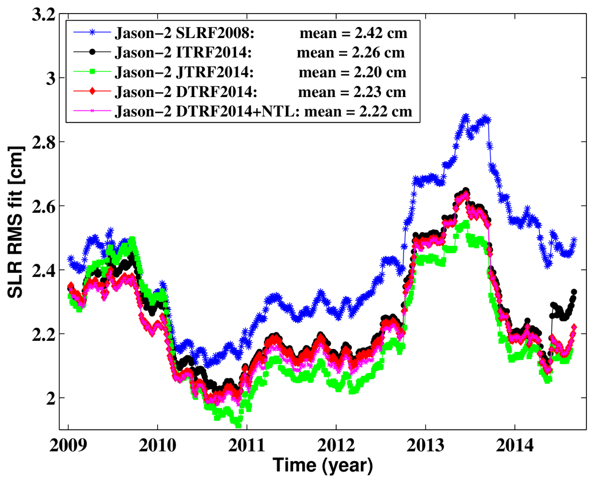

Fig. 8. 50-week running averages of the RMS fits of SLR observations (in cm) for Jason-2 orbits derived using SLRF2008, ITRF2014, JTRF2014, DTRF2014 linear, and DTRF2014+NTL. The plot for DTRF2014 linear is very close to that one for DTRF2014+NTL and is behind it.

extrapolation of the station velocities determined at the time span until this instant, while station velocities are determined using data until 2015.0 when applying the ITRS realizations released in 2016. These results are in agreement with the increase of RMS fits of Jason-2 SLR observations (Fig. 8) when using SLRF2008 as compared to using three other new ITRS realizations. The three latest ITRS realizations do not indicate an increasing with time scatter of the radial orbit differences for Jason-2 (Fig. 11), but ITRF2014 shows a mean difference of 1.33 and 1.46 mm with respect to JTRF2014 and DTRF2014, respectively. The mean values for JTRF2014 and DTRF2014 agree quite well to each other, and differ by just 0.13 mm.

The RMS values of the radial orbit differences of Jason-2 orbits derived using three new ITRS realizations are $3-4$ mm (Table V), whereas the largest differences up to 5.2 mm are obtained using SLRF2008 and JTRF2014. One gets higher percentage (the last column of this Table) of the radial orbit differences larger than 60 mm (that were excluded from the statistics) for JTRF2014, as for the three other ITRS realizations. The mean absolute radial orbit differences are below 1.5 mm for all ITRS realizations. The following pairs of the ITRS realizations show the smallest (less than 0.2 mm) mean absolute radial orbit differences: ITRF2014 and SLRF2008 (since the procedure of the ITRF2014 generation – combination of solutions – is rather similar to that of ITRF2008, an SLR extension of which is SLRF2008), JTRF2014 and DTRF2014, DTRF2014 and DTRF2014+NTL, and DTRF2014+NTL and JTRF2014, since the DTRF2014

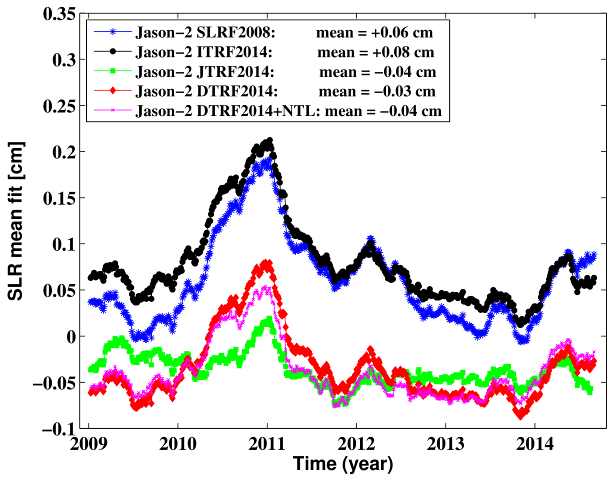

Fig. 9. 50-week running averages of the mean fits of SLR observations (in cm) for Jason-2 orbits derived using SLRF2008, ITRF2014, JTRF2014, DTRF2014 linear, and DTRF2014+NTL.

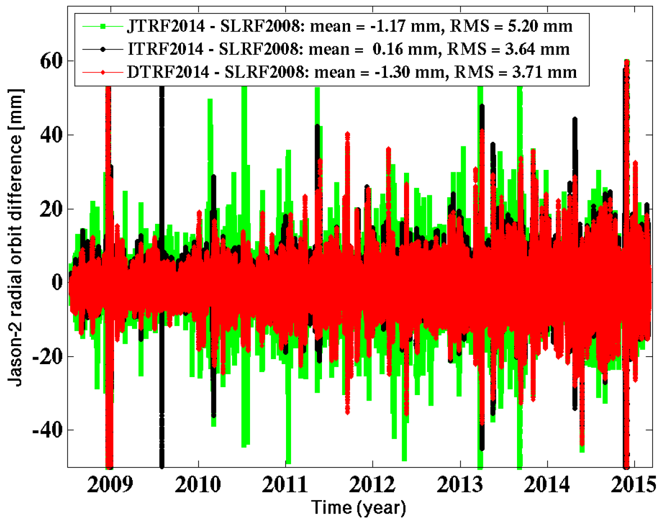

Fig. 10. Radial differences of Jason-2 positions (in mm) derived using DTRF2014, ITRF2014, JTRF2014, and SLRF2008.

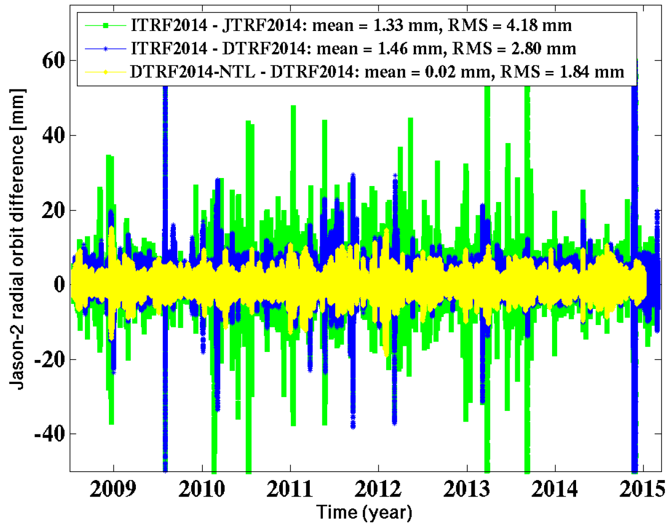

Fig. 11. Radial differences of Jason-2 positions (in mm) derived using DTRF2014, ITRF2014, JTRF2014, and DTRF2014+NTL.

TABLE V

RADIAL ORBIT DIFFERENCES OF JASON-2 ORBITS (IN MM) DERIVED USING VARIOUS TRF REALIZATIONS. THE LAST COLUMN GIVES THE PERCENTAGE OF THE RADIAL ORBIT DIFFERENCES LARGER THAN 60 MM THAT WERE EXCLUDED FROM THE COMPUTATION OF THE MEAN AND RMS VALUES.

Realization differences	Mean (mm)	RMS (mm)	Percentage of outliers (%)
DTRF2014 – SLRF2008	-1.30	3.71	0.009
ITRF2014 – SLRF2008	0.16	3.64	0.020
JTRF2014 – SLRF2008	-1.17	5.20	0.144
ITRF2014 – DTRF2014	1.46	2.80	0.037
ITRF2014 – JTRF2014	1.33	4.18	0.168
JTRF2014 – DTRF2014	0.13	3.62	0.133
DTRF2014+NTL – DTRF2014	0.02	1.84	0.000
DTRF2014+NTL – ITRF2014	-1.43	3.29	0.035
DTRF2014+NTL – JTRF2014	-0.10	3.29	0.133
DTRF2014+NTL – SLRF2008	-1.27	4.07	0.005

and DTRF2014+NTL are produced at the observation level and together with JTRF2014 seem to take more rigorously the seasonal, annual, or semi-annual variations of station positions. This is in a good agreement with Fig. 5 and Fig. 7 showing that the 50-week running averages of the mean fits of SLR observations of LAGEOS-1 and Starlette orbits derived using ITRF2014 are close to those derived using SLRF2008, and those based on JTRF2014 are close to those computed using the DTRF2014+NTL reference frame.

V. IMPACT OF ITRS REALIZATION ON JASON-2 ALTIMETRY RESULTS

In order to analyze the impact of the different ITRS realizations on altimetry-based sea level studies, different orbit solutions are applied to the Jason-2 altimetry data set. The resulting sea surface height (SSH) crossover differences are used to assess the quality of the different orbits. For this purpose, single-satellite crossover differences (SXO) as well as dual-satellite crossover differences are build and analyzed. Moreover, a global multi-mission crossover analysis is applied to estimate radial altimetry errors as well as geographically correlated mean SSH errors. More details on the method and its applications are provided by [8], [30], [31] and [32].

The SXO are computed with a maximum time difference of 10 days. When using the DTRF2014, the mean of all crossover differences yields 0.7 mm with a standard deviation of 59.4 mm. This shows an improvement with respect to the SLRF2008 solution (0.2%). The improvement is slightly larger for JTRF2014 (0.6%) and less for ITRF2014 (0.1%). The results for all orbit solutions are summarized in Table VI.

The changes in radial errors for Jason-2 caused by the usage of different reference frames show differences in the standard deviation of the errors well below 1 mm (Table VII). Compared to the SLRF2008 solution, the DTRF2014 slightly (0.5%) improves the results whereas for ITRF2014 and JTRF2014 small degradations are visible (−0.2% and −0.3%, respectively).

TABLE VI
10-DAY SINGLE-SATELLITE SSH CROSSOVER DIFFERENCES FOR JASON-2 FOR ORBITS BASED ON DIFFERENT REFERENCE FRAME REALIZATIONS.

TRF realization	SXO mean [mm]	SXO std [mm]	Difference w.r.t. SLRF2008 mean [mm]	Difference w.r.t. SLRF2008 std [mm]
SLRF2008	1.00	59.52	–	–
ITRF2014	0.80	59.46	−0.2	−0.1
DTRF2014	0.68	59.40	−0.3	−0.1
DTRF2014+NTL	0.64	59.38	−0.4	−0.1
JTRF2014	0.62	59.16	−0.4	−0.4

TABLE VII
MEAN AND STANDARD DEVIATIONS OF THE RADIAL ERRORS FOR JASON-2 ORBITS BASED ON DIFFERENT REFERENCE FRAME REALIZATIONS

TRF realization	Radial errors mean [mm]	Radial errors std [mm]	Difference w.r.t. SLRF2008 mean [mm]	Difference w.r.t. SLRF2008 std [mm]
SLRF2008	1.943	15.723	–	–
ITRF2014	1.939	15.748	−0.004	+0.025
DTRF2014	1.947	15.649	+0.004	−0.074
JTRF2014	1.937	15.772	−0.006	+0.049

The analysis of the spatial distribution of the radial errors reveals systematic geographically correlated errors (GCE). This error component is most critical for regional sea level studies, since these errors will map directly in the estimated SSH. The scatter of GCE is smallest for the SLRF2008 solution (2.31 mm standard deviation), followed by DTRF2014 (2.36 mm), JTRF2014 (2.41 mm), and ITRF2014 (2.46 mm). Fig. 12 displays Jason-2 GCE computed using DTRF2014 orbit solution (top) as well as the differences to SLRF2008, ITRF2014, and JTRF2014 solutions. The impact of the different reference frames is below 1 mm and in the order of about 10% of the total GCE effect. The main influence is visible in a North-South error distribution indicating differences in the realization of the z-component of the origin.

In order to study the temporal variations in GCE, we divide the radial errors per calendar year in four components (range bias and dx, dy, dz). More details on this method (but for 10-day values) can be found in [8]. In contrast to that paper, we use annual values in order to reduce the noise and to emphasize the long-term behavior of the time series. Fig. 13 displays the temporal variations of differences in the origin realization (dx, dy, dz) between the four orbit solutions under investigation. Whereas almost no differences for x- and y-component are visible, clear offsets in the z-component are evident for Jason-2 orbits derived using DTRF2014 and SLRF2008. However, these seem to be almost constant for the entire Jason-2 time period. Thus, the choice of TRF realization does not significantly influence the large-scale pattern of geographically correlated SSH errors and regional sea level trend computations, but can impact the sea level height.

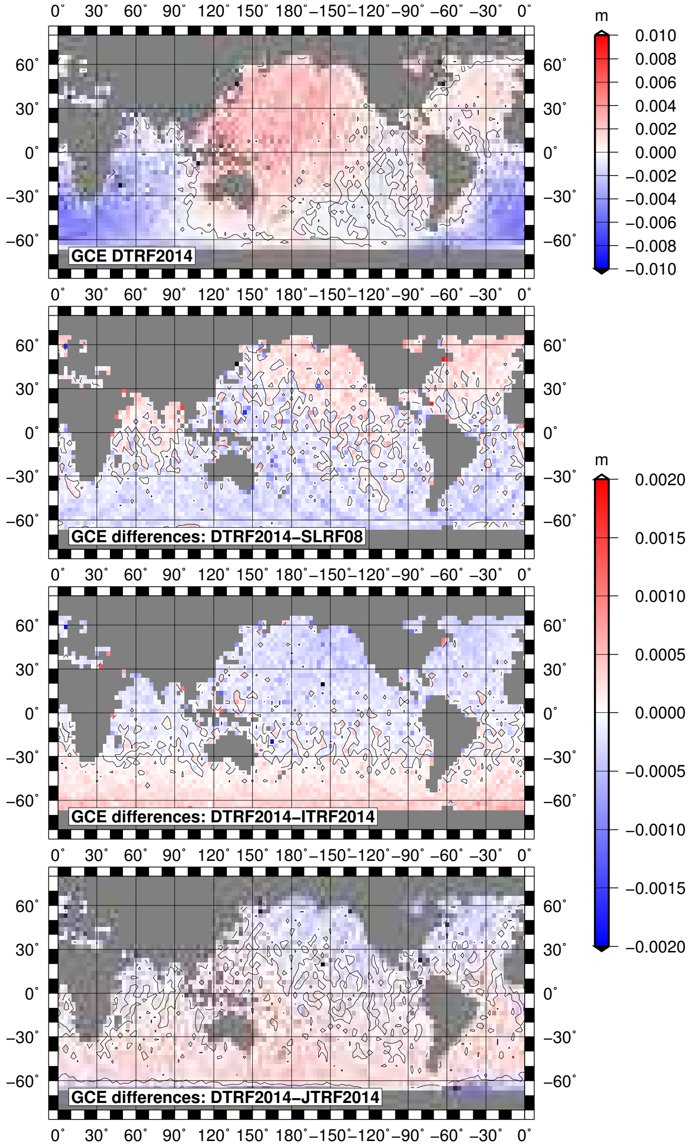

Fig. 12. Geographically correlated mean SSH errors (in m) for Jason-2 using an orbit based on the DTRF2014 reference frame (top) and differences to three other orbit solutions (SLRF2008, ITRF2014, and JTRF2014).

VI. CONCLUSION

In this paper, we have evaluated the ITRS realizations DTRF2014, ITRF2014, and JTRF2014 for precise orbit determination of ten geodetic satellites equipped with SLR retro-reflectors at low and high Earth orbits at a time interval 1993.0 – 2017.0, as compared to using SLRF2008. We have found that the following editing is necessary to the original JTRF2014 realization. One should exclude SLR station Concepcion (CDDIS SOD 74057903, IERS DOMES number 41719M001) after 27 February 2010, since no jump in station position caused by the Maule earthquake ($M_w = 8.8$) is provided for this station in the JTRF2014. Additionally, a solution A with the IERS DOMES number 14001S001 — of two solutions given in the JTRF2014 at the whole time interval — should be used for station Zimmerwald (CDDIS SOD 78106801) before 30 April 1995, and solution B with the DOMES number 14001S007 after this date. After this editing, one gets reasonable results with JTRF2014 for SLR stations.

We have found that SLRF2008 provides, for most satellites, the largest RMS and absolute mean fits of SLR observations and the largest range biases, when estimated. This is especially pronounced at the time interval after 2009.0 as a result of increased uncertainties in station positions due to

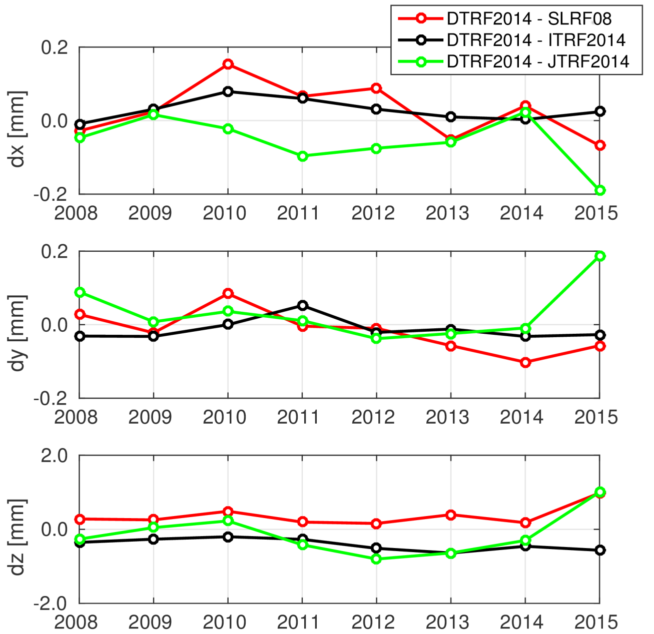

Fig. 13. Temporal variations of differences in the origin realization (in mm) between the four Jason-2 orbit solutions.

the extrapolation of the SLRF2008. Among the new ITRS realizations, the smallest RMS fits and the smallest absolute mean fits of SLR observations are obtained using DTRF2014 linear model with non-tidal loading corrections and JTRF2014. The mean SLR RMS fits reduce (improve), on average over all satellites tested, by 3.0, 3.6, 8.1, and 7.7% at $1993.0 - 2015.0$, when using ITRF2014, DTRF2014, DTRF2014 with non-tidal loading, and JTRF2014 realizations, respectively, as compared to using SLRF2008. The improvement of the RMS fits is even larger at the extrapolation time interval (2015.0–2017.0): 14.0 and 15.5% using ITRF2014 and DTRF2014, respectively. The DTRF2014 provides smallest absolute mean fits of SLR observations in $2015 - 2016$ for all satellites tested. The mean fits of SLR observations computed using ITRF2014 are rather close to those of SLRF2008 and show a $0.2 - 0.3$ mm/y trend at $2001.0 - 2017.0$ indicating an increase (degradation) of the mean fits of the SLR observations.

Using DTRF2014, ITRF2014, and JTRF2014 for Jason-2 POD shows $3 - 4$ mm RMS radial orbit differences, while SLRF2008 indicates $4 - 5$ mm RMS radial orbit differences with respect to the new three TRF realizations. Altimetry analysis of Jason-2 orbits indicates improvements of the scatter and mean of sea surface crossover differences for the orbits derived using JTRF2014 and DTRF2014 with non-tidal loading corrections and, to lower extend, using ITRF2014, as compared to SLRF2008.

The evaluation of the three new ITRS realizations using SLR shows large discrepancies in the height of some stations within the interpolation time interval (1993.0–2015.0) causing systematic differences in estimated range biases of stations. This is especially notable in the extrapolation time interval (2015.0–2017.0), when the station velocities of the ITRF2014 and DTRF2014 solutions already cause differences of several cm for some stations. This systematic effect will increase with time until a next ITRS realization is computed.

From our analysis, we conclude that JTRF2014 (with the editing for SLR stations Conception and Zimmerwald described above) and DTRF2014 with non-tidal loading corrections show the best performance among the ITRS realizations for the satellites tested and are recommended to use until 14 February 2015, while DTRF2014 with non-tidal loading corrections is recommended for use after this date, since JTRF2014 is available only until this date. Certainly the availability of the non-linear station motions (DTRF2014: non-tidal loading, JTRF2014: all signals) is responsible for the better results.

VII. Acknowledgment

The authors are grateful to the Editor Prof. Antonio Plaza and three anonymous reviewers for their comments and useful suggestions that definitely improved the quality of this paper.

References

[1] Z. Altamimi, P. Rebischung, L. Métivier, and X. Collilieux, "ITRF2014: A new release of the International Terrestrial Reference Frame modeling nonlinear station motions," *J. Geophys. Res. Solid Earth*, vol. 121, no. 8, pp. 6109–6131, Aug. 2016.

[2] D. Angermann, M. Seitz, and H. Drewes, "Global terrestrial reference systems and their realizations," in *Sciences of Geodesy II - Innovations and Future Developments,* G. Xu, Ed. Springer, 2013, pp. 97–132.

[3] D. Angermann, T. Gruber, M. Gerstl, R. Heinkelmann, U. Hugentobler, L. Sánchez, and P. Steigenberger, "GGOS Bureau of Products and Standards: Inventory of standards and conventions used for the generation of IAG products," in *The Geodesist's Handbook 2016,*, H. Drewes et al., Eds. *J. Geodesy*, vol. 90, no. 10, pp. 1095–1156, Oct. 2016.

[4] G. Appleby, J. Rodríguez, and Z. Altamimi, "Assessment of the accuracy of global geodetic satellite laser ranging observations and estimated impact on ITRF scale: estimation of systematic errors in LAGEOS observations 1993–2014", *J. Geodesy*, vol. 90, no. 12, pp. 1371-1388, Dec. 2016.

[5] M. Bloßfeld, "The key role of Satellite Laser Ranging towards the integrated estimation of geometry, rotation and gravitational field of the Earth," Dissertation, Technische Universität München and Reihe C der Deutschen Geodätischen Kommission, ISBN: 978-3-7696-5157-7, 2015.

[6] M. Bloßfeld, S. Rudenko, A. Kehm, N. Panadina, H. Muller, D. Angermann, U. Hugentobler, M. Seitz, "Consistent estimation of geodetic parameters from SLR satellite constellation measurements," *J. Geodesy*, 2017, submitted for publication.

[7] M. Bloßfeld, D. Angermann, M. Seitz, "DGFI-TUM analysis and scale investigations of the latest terrestrial reference frame realizations," Proceedings of the Joint Scientific Assembly of IAG and IASPEI in Kobe, Japan (2017), submitted.

[8] W. Bosch, D. Dettmering, and C. Schwatke, "Multi-mission cross-calibration of satellite altimeters: Constructing a long-term data record for global and regional sea level change studies," *Remote Sensing*, vol. 6, no. 3, pp. 2255–2281, Mar. 2014.

[9] B. R. Bowman, W. Tobiska, F. A. Marcos, C. Y. Huang, C. S. Lin, and W. J. Burke, "A new empirical thermospheric density model JB2008 using new solar and geomagnetic indices", *AIAA/AAS Astrodynamics Specialist Conference,* Honolulu, Hawaii, 18–21 Aug. 2008. [Online]. Available: http://sol.spacenvironment.net/jb2008/pubs/AIAA_2008-6438_JB2008_Model.pdf.

[10] I. Ciufolini, A. Paolozzi, E. C. Pavlis, R. Koenig, J. Ries, V. Gurzadyan, R. Matzner, R. Penrose, G. Sindoni, C. Paris, H. Khachatryan, and S. Mirzoyan, "A test of general relativity using the LARES and LAGEOS satellites and a GRACE Earth gravity model", *Eur. Phys. J. C*, vol. 76, no. 3, art. 120, Mar. 2016.

[11] S. D. Desai, "Observing the pole tide with satellite altimetry," *J. Geophys. Res.,* vol. 107, no. C11, pp. 7-1–7-13, Nov. 2002.

[12] J. M. Dow, R. E. Neilan, and C. Rizos, "The International GNSS Service in a changing landscape of Global Navigation Satellite Systems," *J. Geodesy*, vol. 83, no. 3–4, pp. 191-198, Mar. 2009.

[13] C. Förste, S. Bruinsma, R. Shako, J.-C. Marty, F. Flechtner, O. Abrikosov, C. Dahle, J.-M. Lemoine, H. Neumayer, R. Biancale, and the EIGEN team, "EIGEN-6 - A new combined global gravity field model including GOCE data from the collaboration of GFZ Potsdam and GRGS Toulouse", Geophysical Research Abstracts, vol. 13, EGU2011-3242-2, 2011, EGU General Assembly 2011.

[14] W. M. Folkner, J. G. Williams, and D. H. Boggs, "The Planetary and Lunar Ephemeris DE421," The Interplanetary Netw., Jet Propulsion Laboratory, Nat. Aeronautics Space Administration, Pasadena, CA, USA, Tech. Rep. 42-178, Aug. 2009, pp. 1–34. [Online]. Available: http://ipnpr.jpl.nasa.gov/progress_report/42-178/178C.pdf

[15] M. Gerstl, "Parameterschätzung in DOGS-OC," In: DGFI Interner Bericht, MG/01/1996/DGFI, 2nd edition (in German), 1997.

[16] Ch. Haberkorn, M. Bloßfeld, J. Bouman, M. Fuchs, and M. Schmidt, "Towards a consistent estimation of the Earths gravity field by combining normal equation matrices from GRACE and SLR", in C. Rizos, P. Willis (eds.), IAG 150 Years, International Association of Geodesy Symposia 143, 2015, pp. 375–381.

[17] A. E. Hedin, "MSIS-86 thermospheric model," *J. Geophys. Res.,* vol. 92, no. A5, pp. 4649-4662, May 1987.

[18] E. Kalnay et al., "The NCEP/NCAR 40-Year Reanalysis Project," *Bullet. Amer. Meteorol. Soc.,* vol. 77, no. 3, pp. 437–471, Mar. 1996.

[19] P. J. Knocke, J. C. Ries, and B. D. Tapley, "Earth radiation pressure effects on satellites," in *Proc. AIAA/AAS Astrodynamics Conference.* Am. Inst. Aeron. Astronaut., Washington, D.C., USA, 1988, pp. 577-587.

[20] A. S. Konopliv, S. W. Asmar, E. Carranza, W. L. Sjogren, and D.-N. Yuan, "Recent gravity models as a result of the Lunar Prospector Mission," *Icarus*, vol. 150, no. 1, pp. 1-18, Mar. 2001.

[21] V. Luceri, E. C. Pavlis, B. Pace, D. Knig, M. Kuzmicz-Cieslak, and G. Bianco, "Overview of the ILRS Contribution to the Development of ITRF2013", in "REFAG 2014. Proc. IAG Commission 1 Symposium, Kirchberg, Luxembourg, 13–17 October, 2014", IAG SYMPOSIA, vol. 146, T. van Dam (ed.), Springer International Publishing, Switzerland, 2015, pp. 101–108.

[22] T. Otsubo, and G. M. Appleby, "System-dependent center-of-mass correction for spherical geodetic satellites," *J. Geophys. Res.*, vol. 108, no. B4, 2201, Apr. 2003.

[23] T. Otsubo, R. Sherwood, G. Appleby, and R. Neubert, "Center-of-mass corrections for sub-cm-precision laser-ranging targets: Starlette, Stella and LARES", *J Geodesy*, vol. 89, no. 4, pp. 303-312, Apr. 2015.

[24] E. C. Pavlis, "SLRF2008: The ILRS reference frame for SLR POD contributed to ITRF2008", *Ocean Surface Topography Science Team 2009 meeting,* Seattle, WA, June 22–24, 2009. [Online]. Available: http://www.aviso.oceanobs.com/fileadmin/documents/OSTST/2009/poster/Pavlis_2.pdf.

[25] M. R. Pearlman, J. J. Degnan, and J. M. Bosworth, "The International Laser Ranging Service," *Adv. Space Res.*, vol. 30, no. 2, pp. 135–143, Jul. 2002.

[26] G. Petit and B. Luzum, Eds. *IERS Conventions (2010), IERS Technical Note No. 36.* Frankfurt am Main, Germany: Verlag des Bundesamts für Kartographie und Geodäsie, 2010.

[27] G. D. Quartly, J.-F. Legeais, M. Ablain, L. Zawadzki, M. J. Fernandes, S. Rudenko, L. Carrere, P. N. Garcia, P. Cipollini, O. B. Andersen, J.-C. Poisson, S. Mbajon Njiche, A. Cazenave, and J. Benveniste, "A new phase in the production of quality-controlled sea level data," *Earth Syst. Sci. Data*, vol. 9, no. 2, pp. 557–572, Aug. 2017.

[28] R. D. Ray and R. M. Ponte, "Barometric tides from ECMWF operational analyses," *Ann. Geophys.,* vol. 21, no. 8, pp. 1897–1910, Aug. 2003.

[29] M. Rodell et al., "The Global Land Data Assimilation System," *B. Am. Meteorol. Soc.,* vol. 85, no. 3, pp. 381–394, Mar. 2004.

[30] S. Rudenko, D. Dettmering, S. Esselborn, T. Schöne, C. Förste, J.-M. Lemoine, M. Ablain, D. Alexandre, and K.-H. Neumayer, "Influence of time variable geopotential models on precise orbits of altimetry satellites, global and regional mean sea level trends," *Adv. Space Res.*, vol. 54, no. 1, pp. 92–118, Jul. 2014.

[31] S. Rudenko, D. Dettmering, S. Esselborn, E. Fagiolini, and T. Schöne, "Impact of Atmospheric and Oceanic De-aliasing Level-1B (AOD1B) products on precise orbits of altimetry satellites and altimetry results," *Geophys. J. Int.*, vol. 204, no. 3, pp. 1695–1702, Feb. 2016.

[32] S. Rudenko, K.-H. Neumayer, D. Dettmering, S. Esselborn, T. Schöne, and J.-C. Raimondo, "Improvements in precise orbits of altimetry satellites and their impact on mean sea level monitoring," *IEEE T. on Geosci. Remote,*, vol. 55, no. 6, pp. 3382–3395, Jun. 2017.

[33] R. Savcenko and W. Bosch, "EOT11a – Empirical ocean tide model from multi-mission satellite altimetry," Deutsches Geodätisches Forschungsinstitut, Munich, Germany, Tech. Rep. No. 89, 2012, pp. 1–49. [Online]. Available: https://mediatum.ub.tum.de/doc/1300842/1300842.pdf

[34] H. Schuh and D. Behrend, "VLBI: A fascinating technique for geodesy and astrometry", *J. Geodyn.*, vol. 61, pp. 68-80, Oct. 2012.

[35] M. Seitz, D. Angermann, M. Bloßfeld, H. Drewes, and M. Gerstl, "The 2008 DGFI realization of the ITRS: DTRF2008," *J. Geodesy*, vol. 86, no. 12, pp. 1097–1123, Dec. 2012.

[36] M. Seitz, M. Bloßfeld, D. Angermann, R. Schmid, M. Gerstl, and F. Seitz, "The new DGFI-TUM realization of the ITRS: DTRF2014 (data)," Deutsches Geodätisches Forschungsinstitut, Munich, DOI:10.1594/PANGAEA.864046, 2016 (Open Access).

[37] P. Willis, H. Fagard, P- Ferrage, F.G. Lemoine, C.E. Noll, R. Noomen, M. Otten, J.C. Ries, M. Rothacher, L. Soudarin, G. Tavernier, and J.J. Valette, "The International DORIS Service (IDS): Toward maturity," in DORIS: Scientific Applications in Geodesy and Geodynamics, P. Willis (Ed.), *Adv. Space Res.*, vol. 45, no. 12, pp. 1408-1420, Jun. 2010.

[38] X. Wu, C. Abbondanza, Z. Altamimi, T. M. Chin, X. Collilieux, R. S. Gross, M. B. Heflin, Y. Jiang, and J. W. Parker, "KALREF-a Kalman filter and time series approach to the International Terrestrial Reference Frame realization," *J. Geophys. Res. Solid Earth*, vol. 120, no. 5, pp. 3775-3802, May 2015.

[39] N. P. Zelensky, F. G. Lemoine, D. S. Chinn, S. Melachroinos, B. D. Beckley, J. W. Beall, and O. Bordyugov, "Estimated SLR station position and network frame sensitivity to time-varying gravity," *J. Geodesy*, vol. 88, no. 6, pp. 517-537, Jun 2014.